

2nd CIRP 2nd CIRP Conference on Surface Integrity (CSI)

Evolution of residual stresses induced by machining in a Nickel based alloy under static loading at room temperature

A. Madariaga^{a*}, P.J Arrazola^a, J.A. Esnaola^a, J. Ruiz-Hervias^b, P. Muñoz^b

^a Faculty of Engineering, Mondragon University, Loramendi 4, Arrasate 20500, Spain

^b Departamento Ciencia de Materiales, ETSI Caminos, Universidad Politécnica de Madrid, c/ Profesor Aranguren s/n, Madrid 28040, Spain

* Corresponding author. Tel.: +34 943 79 47 00; fax: +34 943 79 15 36. E-mail address: amadariaga@mondragon.edu

Abstract

Tensile residual stresses are very often generated on the surface when machining nickel alloys. In order to determine their influence on the final mechanical behaviour of the component residual stress stability should be considered. In the present work the evolution of residual stresses induced by machining in Inconel 718 under static loading at room temperature has been studied. An Inconel 718 disc has been face turned and specimens for tensile tests have been extracted from the disc. Then surface residual stresses have been measured by X-ray diffraction for initial state and different loading levels. Finally, a finite element model has been fitted to experimental results and the study has been extended for more loading conditions. For the studied case, it has been observed that tensile residual stresses remain stable when applying elastic loads but they increase at higher loads close to the yield stress of the material.

© 2014 The Authors. Published by Elsevier B.V. Open access under [CC BY-NC-ND license](https://creativecommons.org/licenses/by-nc-nd/4.0/).

Selection and peer-review under responsibility of The International Scientific Committee of the “2nd Conference on Surface Integrity” in the person of the Conference Chair Prof Dragos Axinte dragos.axinte@nottingham.ac.uk

Keywords: Residual Stress; Nickel alloy; Machining

1. Introduction

Nickel based and titanium alloys are the most used in the aerospace industry as they offer higher mechanical strength, chemical resistance and thermal conductivity than steels [1]. However, due to these excellent properties, these superalloys are very difficult to machine and the final surface integrity of a machined component can be affected. In fact, over the last decade many research studies have been focused on workpiece surface integrity and functional performance [2] and extent literature reviews overviewing different parameters of the surface integrity of machined nickel and titanium alloys have been carried out [1,3].

Among the different parameters that characterize the final surface integrity of a workpiece, residual stresses induced during machining have covered remarkable attention. Usually, when machining nickel and titanium alloys, tensile stresses are generated on the surface which can reduce the fatigue life of a part [4]. This is an

important aspect to be considered when manufacturing critical components. Nevertheless, residual stresses can vary along the lifetime and their stability should be analyzed in order to quantify their real influence on the component behavior [5]. Under the application of mechanical or/and thermal energy, elastic deformations related to residual stresses can be relaxed if they are transformed into plastic deformations [5]. Basically, residual stresses can be modified due to mechanical loads (static or cyclic), thermal exposure or crack extension [6]. In 2007, McClung carried out a literature survey about the stability of residual stresses induced by shot peening and similar surface treatments, cold expansion of holes, welding and machining processes, observing very few researches about machining [6].

The nickel based alloy Inconel 718 has been selected for this study, which is used 50% by weight in the case of modern engines [7]. Several authors have already studied the stability of residual stresses generated in Inconel 718. Prevey et al. [8] analyzed thermal relaxation of residual stresses induced by shot peening,

gravity peening and laser shock peening. They found considerable relaxation of residual stresses even in short thermal exposures (≈ 10 min) and the relaxation also showed adependence with the percentage of cold work generated by the mechanical treatment. More recently, Hoffmeister et al. [9] studied the thermal relaxation of compressive residual stresses induced by shot peening, and propounded a modified Zener-Wert-Avrami-equation to determine residual stress relaxation for different time exposures and temperatures. On the other hand, Zhuang and Halford [10] carried out an interesting work by finite element method to finally obtain an analytical model capable to predict residual stress relaxation under cyclic mechanical loads. They analyzed the relaxation of residual stresses induced by shot peening, laser shock peening and low plasticity burnishing, demonstrating that it depends on: initial residual stress state, amount of cold work, cyclic load amplitude and mean value, number of cycles and material strain-stress behavior. In one of the latest works, Hoffmeister et al. [11] analyzed residual stress relaxation of shot peened Inconel 718 specimens after isothermal static and cyclic loading. They observed that compressive residual stresses relaxed under static loading until tensile residual stresses were built and during cyclic loading residual stresses relaxed almost completely in the first cycle. It can be concluded there are no studies about the stability of residual stresses generated by machining which are usually tensile on the surface in contrast to compressive residual stresses induced by peening treatments.

The aim of the present paper is to analyze the stability of residual stresses generated by machining in Inconel 718 under mechanical static loading at room temperature. For this purpose an Inconel 718 disc has been face turned and specimens extracted from the disc have been loaded at different stress levels. Initial stresses and final residual stresses have been measured by X-ray diffraction. Finally, a finite element model has been fitted to experimental results and the study has been extended for more loading conditions.

2. Materials and experiments

Inconel 718 rolled sheet with average grain size ($G=7$) and hardened by precipitation was selected for this study. The chemical composition of the material supplied by the manufacturer can be observed in table 1.

Table 1. Chemical composition of Inconel 718 rolled, supplied by the manufacturer

C	Mn	Fe	S	Si	Cu
0.054	0.24	Bal	<0.002	0.1	0.08
Ni	Cr	P	Ti	N	Mo
53.1	18.4	<0.005	0.97		3.06

Table 2. Cutting conditions

Cutting conditions	Cutting speed (m/min)	70
	Feed rate (mm/rev)	0.4
	Depth of cut (mm)	0.3
	Coolant	yes
Tool	Tool insert	Dog bone shape WC coated
	Rake angle ($^{\circ}$)	0
	Clearance angle ($^{\circ}$)	7
	Cutting edge inclination angle ($^{\circ}$)	0
	Cutting edge radius (μm)	30 \pm 5
	Nose radius (mm)	4

As it is schematically represented in Fig. 1, upper and lower intermediate surfaces (grey area) of a 10 mm thick ring shape part was face turned in a Danobat vertical lathe, reducing the thickness of this region to 4 mm. The cutting conditions employed in the present study to machine the ring shape part are summed up in table 2. Both surfaces were machined with coolant and applying the same working conditions: cutting speed (70 m/min), feed rate (0.4 mm/rev) and depth of cut (0.3 mm). A 4 mm nose radius dog bone shape fresh WC coated tool was used to machine each surface. Then, specimens, whose longitudinal axis was aligned with the radial direction of the machined disc, were extracted by electro discharge machining to perform subsequent tensile tests.

First of all, tensile test at room temperature were carried out to obtain the material's strain-stress curve and determine material's yield stress (1180 MPa) to use it as reference in the later tests. Then interrupted tensile tests were carried out in three specimens to study residual stress stability. Each specimen was loaded in tension at room temperature to reach a maximum stress level over the yield stress in the calibrated section (1220 MPa, 1300 MPa and 1350 MPa) and then unloaded. Before performing these tests, initial surface residual stresses (σ_{RS0}) were measured on both surfaces in the middle of the specimens (point A) in the axial direction as it is shown in Fig. 2. Final surface residual stresses (σ_{RSf}) were measured at the same points in the tested specimens. In the specimen loaded up to 1220 MPa additional measurements were done at points B and C, where the nominal stress was kept below the yield stress.

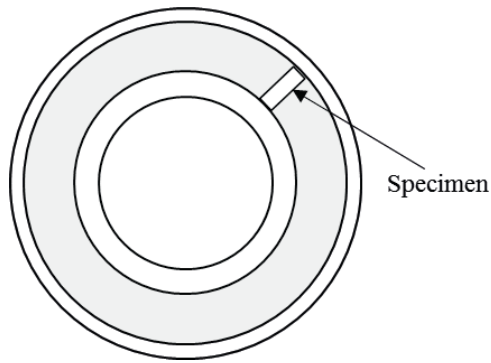


Fig. 1. Schematic representation of the machined ring shape disc

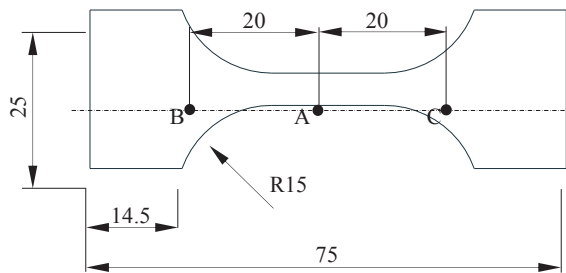


Fig. 2. Specimen geometry and residual stress measurements points

Initial and final surface residual stresses were measured in the longitudinal direction by X-ray diffraction technique, employing a PROTO iXRD diffractometer and analyzed with XrdWin software. The tube voltage was 20 kV and the tube current 4 mA. The diffraction plane was $\{3\ 1\ 1\}$ and a 2 mm diameter area was irradiated by a $\text{MnK}\alpha$ ($\lambda=2.103\ \text{\AA}$) radiation. Measurements were carried out in mode Ω with 7 inclinations. The diffraction elastic constants used in the measurements were these: $-S_1=1.61\cdot 10^{-6}\ [\text{MPa}^{-1}]$, $\frac{1}{2} S_2=7.14\cdot 10^{-6}\ [\text{MPa}^{-1}]$.

3. Finite element model

The surface-core model is a simple model that enables to analyze the uniaxial residual stress stability [12]. The model is based on a prismatic rod which is divided into a thinner surface layer and a core region. State-specific strain-stress properties and initial surface residual stresses are assigned to the surface layer and raw material's strain-stress properties to the core region. Axial surface and core residual stresses are assumed to be effective within these regions and both regions are submitted to equal total strain when loading. This model has been employed in numerous research works to study the relaxation of compressive residual stresses induced by shot peening and similar treatments under mechanical

loads [13]. Recently, Hoffmeister *et al.* [11], used the surface-core model to analyze residual stress relaxation of shot peened Inconel 718 specimens after isothermal static and cyclic loading, observing good agreement between experimental and calculated results.

In the present work the surface-core model was implemented in the commercial Abaqus Standard finite element software to analyze surface residual stress stability (the use of multiple-layer model is required to study residual stress variations in depth). For that purpose, assuming plane stress behavior, a small longitudinal section (2 mm long and 2 mm high) of the calibrated region of the specimen was modeled. As it is shown in Fig. 3 the load was applied in the longitudinal direction on the left side and longitudinal movement was restricted on the right side whilst symmetry conditions were employed on the bottom side. This section was divided into a 4 μm thick surface layer and the core region. The strain-stress response of the material previously obtained in rupture tensile tests (see Fig. 5) was assigned to the core region. Nickel based alloys such as Inconel 718 are prone to work-hardened when machining [1]. As reported by Pawade *et al.* [14] the local yield stress of the machined surface, depending on the working conditions, can be increased even up to 1.8 times the yield stress of the core material. The yield stress of the surface layer used in the present work was estimated based on full width at half medium values obtained by authors in a previous study [15], where residual stresses generated in Inconel 718 under similar working conditions were measured by X-ray diffraction method. Taking into account the methodology developed by Nobre and co-workers [16], the new yield stress of the surface layer was predicted using equation (1), where σ_y is the new yield stress, σ_{y0} is the initial yield stress, ΔH is the change in the diffraction width, H_0 is the initial diffraction width and γ is a material dependent constant.

$$\sigma_y = \sigma_{y0} \left(1 + \gamma \frac{\Delta H}{H_0} \right) \quad (1)$$

On the other hand, experimentally measured initial surface residual stress (average value) was introduced in the surface layer in the longitudinal direction assuming that they were homogenous throughout this layer. In Fig. 4 a small region of the finite element model is shown, where initial surface residual stress is only introduced in the surface layer. In order to analyze numerically the surface residual stress stability the model was loaded to 1220 MPa, 1300 MPa and 1350 MPa nominal stress levels and final surface residual stresses were measured in the longitudinal direction after the unloading. Once having fitted the

calculated final residual stresses and experimental results, the study was extended to a wide range of loads.

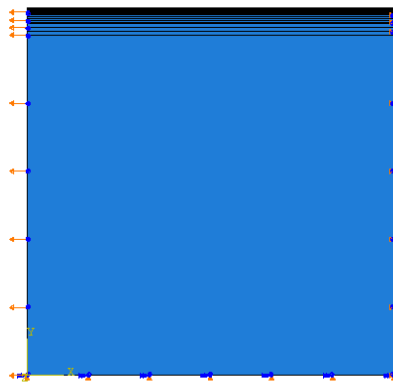


Fig. 3. Finite element model. Boundary and loading conditions

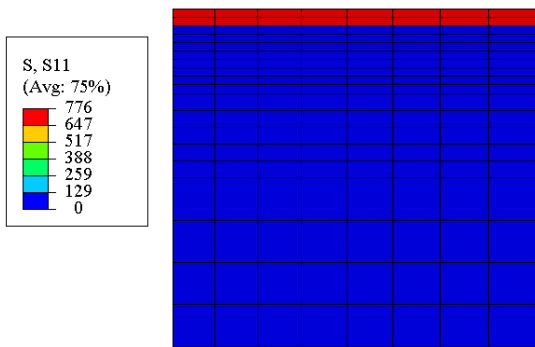


Fig. 4. Detail of initial surface residual stress

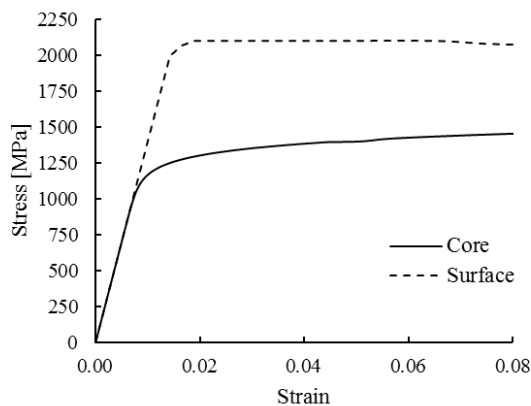


Fig. 5. Core and surface material's strain-stress curves

4. Results and discussion

4.1. Experimental results

Initial surface residual stresses generated by the machining process were measured in the longitudinal

direction at different points as explained in section 2. They gave an average value of 776 MPa, which is 66% of the yield stress of the core material. Although it depends on the cutting conditions, tensile stresses are usually induced on the surface of Nickel based alloys when turning. Residual stresses introduced by machining process depend on the thermal effect, which induces more tensile stresses, and mechanical effect associated to machining forces, which leads to more compressive stresses. Therefore, in the present work the thermal effect prevailed over the mechanical effect.

Fig.6 and Fig. 7 show the residual stress variations $\Delta\sigma_{RS} = \sigma_{RS0} - \sigma_{RSf}$ regarding applied stress and core plastic strain respectively. As it can be seen in Fig. 6 surface residual stresses on the middle of the specimen increased almost 100 MPa when applying 1220 MPa and very little plastic deformation of the core occurred (see Fig. 5). For this loading condition surface residual stresses at points B and C of the specimen (see Fig. 2) did not vary at all, as neither the surface nor the core were deformed plastically. When loading the specimen up to 1300 MPa again the surface residual stress increased but less (around 70 MPa). Nevertheless for the maximum applied load used in the present study (1350 MPa), the surface residual stress was reduced 170 MPa.

The evolution of the surface residual stresses found in the present work has also been observed by other researchers, especially when analyzing the stability of compressive residual stresses induced by peening treatments. Some of these works are summed up by Schulze [13]. For example, initial compressive residual stresses in shot peened AISI4140, TiAl6V5 or AlCu5Mg2 rapidly became tensile once the applied load reached a certain tensile stress value, but by increasing the load even more residual stresses began to decrease and finally turned to compressive. This evolution of surface residual stresses under tensile loading depends on the relations of yield strengths and work-hardening rates in the surface layer and the core [13]. Initially residual stresses became more tensile because the core yielded first and after that residual stresses became even more tensile as the surface work-hardening rate was greater. Finally, residual stresses reduced at higher loads, associated to a greater work-hardening rate of the core material.

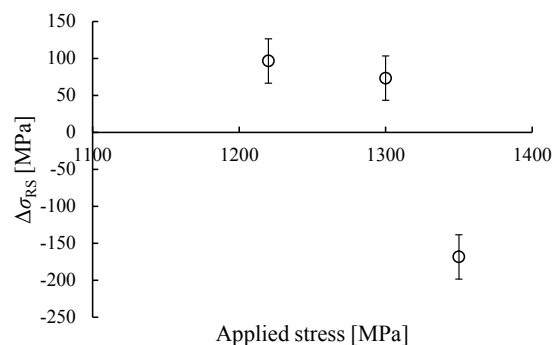


Fig. 6. Surface residual stress variation under different applied loads

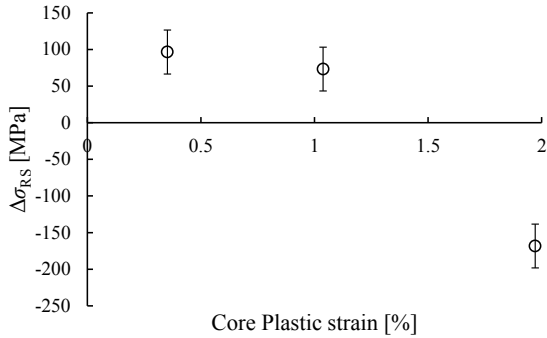


Fig. 7. Surface residual stress variation vs plastic strain generated in the core

4.2. Numerical results

In Fig. 8 surface residual stresses obtained by the finite element model for a wide load range and surface residual stresses measured by X-ray diffraction method (open circles) are compared. Two material models were used to calculate final surface residual stresses. One model, as explained in section 3, employed different properties in the core and in the surface, as it was work-hardened during machining. The second model, built to complement the discussion section, considered the strain-stress properties of the core for the whole model. The values calculated with the first model are represented by continuous line and the stresses determined with the second model are drawn by an interrupted line. In addition, Fig.9 depicts the difference between the plastic strain generated in the core region ($\epsilon_{p,core}$) and the plastic strain induced in the surface layer ($\epsilon_{p,surf}$) for the studied applied load range.

Residual stress changes that occur in the surface layer can be explained by equations (1) and (2). Initial residual stresses vary if there is a difference $\Delta\epsilon_p$ between the core region plastic strain and surface layer plastic strain. As both, surface layer and core region, must experience the same deformation, surface layer is elastically stretched ($\Delta\epsilon_{e,surf}$) and core is elastically compressed ($-\Delta\epsilon_{e,core}$) if $\Delta\epsilon_p > 0$. Consequently, the final surface residual stress increases by summing $E\Delta\epsilon_{e,surf}$ to the initial surface residual stresses. If $\Delta\epsilon_p < 0$, the surface layer is elastically compressed and final surface residual stress is lower than initial stress.

$$\Delta\epsilon_p = \epsilon_{p,core} - \epsilon_{p,surf} = -\Delta\epsilon_{e,core} + \Delta\epsilon_{e,surf} \tag{2}$$

$$\sigma_{RSf} = \sigma_{RS0} + E\Delta\epsilon_{e,surf} \tag{3}$$

The model which considered the surface work-hardened layer was capable of reproducing the evolution of surface residual stresses. As it can be seen in Fig. 8 initial surface residual stresses remain invariable until a 1180 MPa nominal load is applied. Initially, the core becomes yielding whilst the surface layer is within the elastic region, and thus, the surface layer must be stretched to fulfill deformation compatibility after unloading (see Fig. 9). When increasing the applied load over 1180 MPa, the plastic strain difference $\Delta\epsilon_p$ increases and therefore, residual stress becomes higher until a maximum tensile stress is reached. After that, residual stress becomes to decrease, as do $\Delta\epsilon_p$. Finally, at higher loads, the plastic strain difference $\Delta\epsilon_p$ turns negative and final surface residual stress becomes lower than initial stress. This occurs due to differences in the work-hardening rate, at higher loads the core exhibits a higher work-hardening rate.

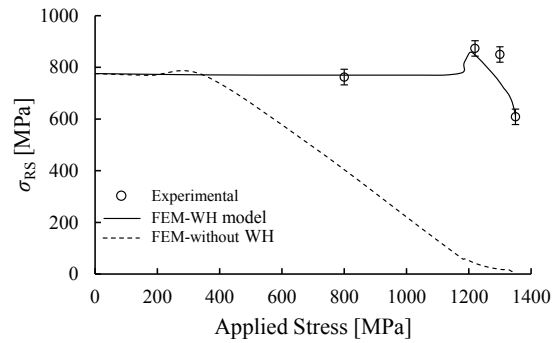


Fig. 8. Surface residual stress evolution under different loads

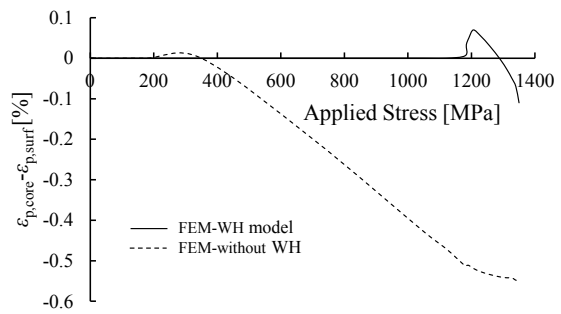


Fig. 9. Core-Surface plastic strain difference under different loads

The mechanical properties of the surface layer are crucial to determine accurately the evolution of residual stresses under different static loads. In order to clarify this point results obtained by the two finite element models are compared in Fig. 8. It clearly shows that if the same material properties are attributed to the whole

model numerical results differ substantially from the experimental data. Indeed, if same properties are used in both regions, residual stresses are predicted to remain constant until a 420 MPa load is applied. When applying this load, the sum of the initial stress and the applied load is higher than the yield stress and the surface becomes yielding whilst the core is elastically deformed ($\Delta\epsilon_p < 0$) as can be seen in Fig.9. Therefore, surface residual stresses decrease for higher applied loads, as the plastic strain difference magnitude increases, and they are almost removed when the applied load exceeds the yield stress of the core material.

5. Conclusions

The main conclusions of the present work are the following:

- For the studied case, initial tensile surface residual stress became even more tensile when applying loads higher than the material yield strength. This occurs due to the higher plastic strain suffered by the core compare to the surface layer. Nevertheless, a shift was observed at the highest applied load (1350 MPa) and initial residual stress was relaxed about 170 MPa as at higher loads the surface plastic strain was greater than the core's. This particular behavior is associated to the different work-hardening rate of the surface layer and the core.
- A finite element model based on the surface-core model has been built and compared with experimental data. Results have shown good agreement, and therefore the model is capable of explaining the evolution of surface residual stresses under static loading.
- The importance of attributing local stress-strain properties to the surface. If the same material is used for the whole model, deformations generated in the surface layer and core region will not be calculated accurately and consequently residual stress predictions will be very far from the experiments.

Acknowledgements

The authors wish to acknowledge the department of material science of the ETSI Caminos of UPM Madrid for their support in the measurements of residual stresses.

The authors thank the Basque and Spanish Governments for the financial support given to the projects PROFUTURE I and II (codes IE 10-271 and IE11-308) and InProRet (code IE12-342), InProRet II (code IE13-XXX) and METINCOX (DPI2009-14286-C02-0 and PI-2010-11).

References

- [1] Ulutan, D., Ozel, T., 2011. Machining induced surface integrity in titanium and nickel alloys: a review. *International Journal of Machine Tools and Manufacture* 51(3), pp. 250-280.
- [2] Jawahir, I. S., Brinksmeier, E., M'Saoubi, R., Aspinwall, D.K., Outeiro, J.C., Meyer, D., Umbrello, D., Jayal, A.D., 2011. Surface integrity in material removal processes: Recent advances. *CIRP Annals-Manufacturing Technology* 60(2), pp. 603-626.
- [3] M'Saoubi, R., Outeiro, J.C., Chandrasekaran, H., Dillon Jr., O.W., 2008. A review of surface integrity in machining and its impact on functional performance and life of machined products. *International Journal of Sustainable Manufacturing* 1(1), pp. 203-236.
- [4] García Navas, V., Gonzalo, O., Bengoetxea, I., 2012. Effect of cutting parameters in the surface residual stresses generated by turning in AISI 4340 steel. *International Journal of Machine Tools and Manufacture* 61, pp. 48-57.
- [5] Totten, G. E., ed., 2002. *Handbook of residual stress and deformation of steel*. ASM international.
- [6] McClung, R. C., 2007. A literature survey on the stability and significance of residual stresses during fatigue. *Fatigue & Fracture of Engineering Materials & Structures* 30(3), pp. 173-205.
- [7] Thakur, D. G., Ramamoorthy, B., Vijayaraghavan, L., 2009. Machinability investigation of Inconel 718 in high-speed turning. *The International Journal of Advanced Manufacturing Technology* 45(5-6), pp. 421-429.
- [8] Prev y, P., Hombach, D., Mason, P., 1998. Thermal residual stress relaxation and distortion in surface enhanced gas turbine engine components. *Lambda research Cincinnati OH*.
- [9] Hoffmeister, J., Schulze, V., Wanner, A., Hessert, R., Koenig, G., 2008. Thermal Relaxation of Residual Stresses induced by Shot Peening in IN718. In *Proceedings of the 10th International Conference on Shot Peening*, Tokyo, Japan, pp. 157-162.
- [10] Zhuang, W. Z., Halford, G.R., 2001. Investigation of residual stress relaxation under cyclic load. *International Journal of Fatigue* 23, pp. 31-37.
- [11] Hoffmeister, J., Schulze, V., Hessert, R., Koenig, G., 2012. Residual stresses under quasi-static and cyclic loading in shot peened Inconel 718. *International Journal of Materials Research* 103(1), pp. 66-72.
- [12] Vohringer, O., 1987. *Relaxation of residual stresses by annealing or mechanical treatment*. Pergamon Press, *Advances in Surface Treatments. Technology--Applications--Effects* 4, pp. 367-396.
- [13] Schulze, V., 2006. *Modern mechanical surface treatment*. Wiley.com.
- [14] Pawade, R. S., Joshi, S.S., Brahmanekar, P.K., 2008. Effect of machining parameters and cutting edge geometry on surface integrity of high-speed turned Inconel 718. *International Journal of Machine Tools and Manufacture* 48(1), pp. 15-28.
- [15] Kortabarria, A., Madariaga, A., Fernandez, E., Esnaola, J.A., Arrazola, P.J., 2011. A comparative study of residual stress profiles on Inconel 718 induced by dry face turning. *Procedia Engineering* 19, pp. 228-234.
- [16] Nobre, J. P., Dias, A.M., Kormmeier, M., 2004. An empirical methodology to estimate a local yield stress in work-hardened surface layers. *Experimental mechanics* 44(1), pp. 76-84.